

Comparing Scaffold-Free and Fibrin-Based Adipose-Derived Stromal Cell Constructs for Adipose Tissue Engineering: An In Vitro and In Vivo Study

Femke Verseijden,* Sandra J. Posthumus-van Sluijs,* Johan W. van Neck,*
Stefan O. P. Hofer,† Stevan E. R. Hovius,* and Gerjo J. V. M. van Osch‡§

*Department of Plastic and Reconstructive Surgery, Erasmus MC,
University Medical Center Rotterdam, Rotterdam, The Netherlands

†Division of Plastic Surgery, University Health Network, University of Toronto, Toronto, Ontario, Canada

‡Department of Orthopedics, Erasmus MC, University Medical Center Rotterdam, Rotterdam, The Netherlands

§Department of Otorhinolaryngology, Erasmus MC, University Medical Center Rotterdam, Rotterdam, The Netherlands

Success of adipose tissue engineering for soft tissue repair has been limited by insufficient adipogenic differentiation, an unfavorable host response, and insufficient vascularization. In this study, we examined how scaffold-free spheroid and fibrin-based environments impact these parameters in human adipose-derived stromal cell (ASC)-based adipose constructs. ASCs were differentiated in spheroids or fibrin-based constructs. After 7 days, conditioned medium was collected and spheroids/fibrin-based constructs were either harvested or implanted subcutaneously in athymic mice. Following 7 days of implantation, the number of blood vessels in fibrin-based constructs was significantly higher than in spheroids (93 ± 45 vs. 23 ± 11 vessels/mm²) and the inflammatory response to fibrin-based constructs was less severe. The reasons for these results were investigated further in vitro. We found that ASCs in fibrin-based constructs secreted significantly higher levels of the angiogenic factors VEGF and HGF and lower levels of the inflammatory cytokine IL-8. Furthermore, ASCs in fibrin-based constructs secreted significantly higher levels of leptin and showed a 2.5-fold upregulation of the adipogenic transcription factor PPARG and a fourfold to fivefold upregulation of the adipocyte-specific markers FABP4, perilipin, and leptin. These results indicate that fibrin-based ASC constructs are potentially more suitable for ASC-based adipose tissue reconstruction than scaffold-free spheroids.

Key words: Mesenchymal stem cell; Adipose tissue engineering; Fibrin; Cytokines; Inflammation; Angiogenesis

INTRODUCTION

Soft tissue defects due to tumor resection, trauma, deep burns, or congenital deformities require surgical replacement of lost soft tissue to regain shape and/or physiological function. Current surgical procedures to repair soft tissue defects include the use of synthetic implants and adipose tissue transplants. Improved patient outcomes notwithstanding (4,6,13,19) both procedures have their limitations including implant dislocation and toxicity (48), donor site morbidity or deformity (43), and an unsatisfactory long-term outcome due to resorption (12, 33,41,48).

Adipose-derived stromal cell (ASC)-based reconstruction after soft tissue loss promises to restore the shape and volume of the affected site. New human adipose tissue

has been formed in immune-compromised rodents by injection of ASCs (5) or delivery of ASCs in tissue-like structures (10,18,22,36,42,43), but poor survival after transplantation due to ischemia, insufficient adipogenic differentiation, and adverse effects of scaffold materials currently hinder the use of these techniques.

Scaffold-based tissue engineering, although promising, faces several challenges: (1) synthetic scaffolds and extracellular matrix-based xenograft materials elicit a foreign body response, (2) scaffold degradation products may release potentially toxic substances, and (3) scaffold compliance is often different from adipose tissue (21,57).

The generation of three-dimensional tissues that are composed only of cells and their own secreted matrix, also called scaffold-free tissue engineering, addresses

the limitations associated with synthetic and exogenous matrix-based tissues (25,47). Scaffold-free human ASC sheets can be created and stacked to form adipose-like substitutes (50,51). We recently created three-dimensional spherical scaffold-free constructs composed of human ASCs (ASC spheroids) of up to 600 μm in diameter (53). To date, it is unclear whether the use of scaffold-free ASC constructs is advantageous for adipogenesis and/or in vivo engraftment when compared to scaffold-based constructs.

To investigate this, we wanted to compare our scaffold-free methods with another promising method that makes use of scaffolds. Various scaffold materials have been combined with ASCs for adipose tissue engineering purposes (21). Along with collagen (27,40), hyaluronic acid (20), poly(lactic-co-glycolic-acid) (PLGA) (11,42), polyglycolic acid (PGA) (16), Matrigel™ (24), and alginate (18), fibrin has shown a promising scaffold material for generation of adipose tissue (9,45,49,54). Besides that, fibrin is especially an attractive material for clinical use since it could be produced from a patient's own blood, thereby avoiding the risk of a foreign body response (58).

Since the in vivo engraftment of ASC constructs is most of all dependent on ASC survival, a potential successful ASC construct not only supports adipogenesis but also encourages angiogenesis to minimize ASC ischemia and death. As the extracellular environment influences cell behavior (14,46), it is likely that the scaffold(-free) environment will impact important ASC biological features for in vivo engraftment, such as adipogenic differentiation potential and the secretion of adipokines, which include angiogenic and inflammatory factors.

In this study, we examined how scaffold-free spheroid and fibrin-based cultures affect ASC physiology in an adipose tissue engineering setting both in vivo and in vitro. We investigated vessel density and lipid droplet accumulation in constructs in vivo. In addition, we evaluated ASC adipogenic differentiation and the secretion of adipokines by ASCs in scaffold-free spheroid and fibrin-based cultures in vitro.

MATERIALS AND METHODS

Isolation and Culture of ASCs

Subcutaneous abdominal adipose tissue was obtained as leftover material from donors undergoing breast reconstruction surgery with approval of the Erasmus MC Medical Ethical Committee (#MEC-2005-157) and according to the Code of Conduct: "Proper Secondary Use of Human Tissue" (<http://www.federa.org>). Leftover adipose tissue was only used from donors who did not opt-out to such use.

ASCs from three different donors of 56, 58, and 62 years of age were isolated from the adipose tissue using

collagenase type I (Invitrogen, Carlsbad, CA, USA) as previously described (52,53) and grown on basal medium [Dulbecco's modified Eagle's medium 1 g/L glucose (Invitrogen), 10% FCS (fetal calf serum; PAA Laboratories, Pasching, Austria), 10^{-12} M dexamethasone, 10^{-5} M ascorbic acid (both from Sigma-Aldrich, St. Louis, MO, USA), 1% penicillin/streptomycin, 0.5% gentamycin (both from Invitrogen)]. The isolated primary ASCs were grown until they reached 90% confluence. At 90% confluence, adherent cells were released with 0.05% trypsin/ethylenediaminetetraacetic acid (EDTA) and then stored in liquid nitrogen until further use. ASCs at second passage were used in this study.

Formation of Spheroids

ASCs were pooled to a total of 0.5×10^6 cells in 10 ml polypropylene tubes (Techno Plastic Products, Trasadingen, Switzerland) in 350- μl culture medium: human endothelial-SFM (Invitrogen) supplemented with 5% FCS, 20 ng/ml fibroblast growth factor 2 (FGF2), 100 ng/ml epidermal growth factor (EGF), 1% penicillin/streptomycin, and 0.5% gentamycin. After centrifugation at $150 \times g$ for 5 min, cell pellets were incubated overnight in 37°C at 5% CO_2 in a humidified atmosphere to allow spheroid formation. After overnight incubation, the culture medium of the spheroids was replaced by 350 μl of a 1:1 mixture of culture medium and differentiation medium [Dulbecco's modified Eagle's medium 4.5 g/L glucose (Invitrogen), 10% FCS, 1 μM dexamethasone (Sigma-Aldrich), 0.01 mg/ml insulin (Eli Lilly, Houten, The Netherlands), 0.2 mM indomethacin (Sigma-Aldrich), 0.5 mM 3-isobutyl-1-methyl-xanthine (Sigma-Aldrich), 1% penicillin/streptomycin, and 0.5% gentamycin], from now on called the adipogenic medium. Medium was refreshed every other day. At day 7, spheroids were collected for RNA isolation or implantation or cultured for another 48 h on fresh adipogenic medium to analyze secreted angiogenic and inflammatory factors.

Formation of Fibrin-Based Constructs

Fibrin-based constructs were prepared with materials from the fibrin in vitro angiogenesis assay® (Millipore Corporation, Billerica, MA, USA) according to the manufacturer's instructions with some slight modifications. In short, ASCs were suspended in 30 μl of fibrinogen solution at a density of 1.67×10^4 cells/ μl (total of 0.5×10^6 cells per construct). After addition of 20 μl of thrombin solution, the cultures were immediately placed in individual wells of a 96-well plate (Costar®, Corning, Inc.). After gel formation, the plates were incubated at 37°C in 5% CO_2 in a humidified atmosphere for 15 min to ensure polymerization of the gels. Following

polymerization, 350 μ l of culture medium was added to each well. After overnight equilibration, the culture medium was replaced by 350 μ l adipogenic medium. Medium was refreshed every other day. At day 7, fibrin constructs were collected for RNA isolation or implantation or cultured for another 48 h on fresh adipogenic medium to analyze secreted angiogenic and inflammatory factors.

RNA Isolation and Complementary DNA (cDNA) Synthesis

For each of the three ASC donors, 0.5×10^6 second passage undifferentiated ASCs were harvested for RNA isolation. In addition, nine spheroids and nine fibrin constructs were prepared for each of the three ASC donors. The spheroids were fragmented with a pestle on ice and subsequently sheared using an insulin syringe. The fibrin cultures were snap frozen and processed using the Mikro-Dismembrator S[®] (B. Braun Biotech International GmbH, Melsungen, Germany). Total RNA was extracted from undifferentiated ASC, spheroids, and fibrin cultures using Qiazol Lysis Reagent (Qiagen Benelux, Venlo, The Netherlands) and further purified using the RNeasy Micro Kit (Qiagen, Venlo, The Netherlands) with on-column DNA digestion. Total RNA was quantified using a NanoDrop[™] 1000 spectrophotometer (Nanodrop Technologies, Wilmington, DE, USA) according to the manufacturer's instructions, and 250 ng RNA was reverse transcribed into cDNA using the RevertAid[™] First Strand cDNA Synthesis Kit (Fermentas, St. Leon-Rot, Germany).

Quantitative Polymerase Chain Reaction (Q-PCR)

The mRNA levels of the adipogenic markers peroxisome proliferator-activated receptor γ (PPARG), fatty acid binding protein 4 (FABP4), perilipin 1 (PLIN 1), and leptin (LEP), together with β -2-microglobulin (B2M), were analyzed with the ABI PRISM[®] 7000 Sequence Detection System and 7000 System SDS software (ABI, Foster City, CA, USA, www.appliedbiosystems.com), using the Taqman[®] Gene Expression Assays for PPARG (Hs01115510_m1), FABP4 (Hs01086177_m1), PLIN1 (Hs01106927_m1), LEP (Hs00174877_m1), and B2M (Hs00984230_m1) (ABI) according to the manufacturer's instructions. The B2M mRNA levels were analyzed for data normalization.

Conditioned Media Collection and Analysis

On culture day 7, spheroid- and fibrin-based ASC cultures were switched to fresh adipogenic medium and incubated at 37°C and 5% CO₂ for 48 h. Then conditioned media were collected and assayed for the concentration of ASC-secreted inflammatory cytokines, angiogenic factors, and leptin.

Analysis of Inflammatory Cytokines and Angiogenic Factors

A human cytokine inflammation multiplex chemiluminescent ELISA kit (Cat. No. 110451HU, Quansys Biosciences, West Logan, UT, USA) and a human cytokine inflammation multiplex chemiluminescent ELISA kit (cat. no. 150251HU; Quansys Biosciences) were used to assay conditioned and unconditioned medium for the release of the following inflammatory cytokines and angiogenic factors: interleukin-1 α (IL-1 α), IL-1 β , IL-2, IL-4, IL-6, IL-8, IL-10, tumor necrosis factor- α (TNF- α), interferon- γ (IFN- γ), platelet-derived growth factor (PDGF), vascular endothelial growth factor (VEGF), angiopoietin 2 (ANG2), fibroblast growth factor 2 (FGF2), hepatocyte growth factor (HGF), and the tissue inhibitors of metalloproteinases (TIMP): TIMP1, and TIMP2. The multiplex chemiluminescent ELISA kits were performed according to the manufacturer's instructions. The plate was imaged using the Kodak Digital Science[™] Image Station 440CF system (NEN Life Science Products, Inc., Boston, MA, USA) with custom software. Q-view software[®] (Quansys Biosciences) was used for calculation of angiogenic factor concentration using linear regression of the standard curve. As controls, we used both unconditioned medium and medium conditioned on cell-free fibrin gels. Since we measured no differences in growth factor/cytokine secretion between unconditioned and conditioned medium of cell-free fibrin gels, we have combined them in our results as one group referred to as unconditioned medium.

Leptin Quantification

The concentration of leptin in the conditioned medium was measured using a sandwich ELISA kit (Leptin Human ELISA Kit[®], Cat. No. KAC2281, Invitrogen) according to the manufacturer's instructions. The plate was read at 450 nm using a microplate reader (Versamax[®], Molecular Devices, Sunnyvale, CA, USA). The amount of leptin was determined from standard curves provided with the kit.

In Vivo Implantation

For in vivo implantation, three spheroid- and fibrin-based constructs, each initially seeded with 0.5×10^6 ASCs, were created from each of the three donors, resulting in a total of nine ASC spheroids and nine fibrin-based constructs. After 7 days of in vitro culture, the spheroids and fibrin-based constructs were implanted subcutaneously in the left and right scapular area of nine 9-week-old athymic male nude mice (NMRI-nu/nu, Taconic, Hudson, NY, USA). The mice were placed under general anesthesia with 2.5% isoflurane after which two separate 0.5-cm incisions were made through the dorsal skin. Next, two separate subcutaneous pockets were prepared by blunt dissection

of the subcutaneous tissue. One pocket was filled with an ASC spheroid and the other pocket was filled with an ASC seeded fibrin-based construct. Pockets were closed with discontinuous sutures using Mersilk 5-0 (Ethicon, Somerville, NJ, USA). Seven days after implantation, the mice were sacrificed and the constructs retrieved. All animal procedures were approved by the Institutional Animal Experiments Committee of the ErasmusMC (EUR. 1292) (i.e., adherence to the rules prescribed in the national Animals Act, which implements the "Guidelines on the Protection of Experimental Animals" by the Council of Europe, 1986: Directive 86/609/EC).

Histology

Spheroids and fibrin-based constructs harvested before or after 7 days of implantation were embedded in Tissue-Tek (Sakura, Finetek Europe, Zoeterwoude, The Netherlands) and snap frozen or fixed in 10% formalin in PBS followed by embedding in paraffin. Paraffin sections (5 μ m) were deparaffinized and rehydrated. Cryosections (5 μ m) were fixed with 3.7% formalin in deionized water for 1 h.

Vimentin Staining

To distinguish human tissue from mouse tissue in paraffin and cryosections of implanted spheroids and fibrin-based constructs, a monoclonal mouse antihuman vimentin antibody [Clone V9, Cat. No. V6630, 1:40 dilution in PBS/1% BSA (bovine serum albumin), Sigma-Aldrich] was used. To reduce unspecific binding of the secondary goat antimouse antibody (Dako, Glostrup, Denmark) to mouse IgGs, the mouse-on-mouse horse radish peroxidase (HRP)-polymer kit (Biocare Medical, Concord, CA, USA) was used according to the manufacturer's instructions with some slight modifications. In short, antigen retrieval was performed through incubation in Rodent Decloaker[®] (Biocare Medical) for 60 min at 95°C. Nonspecific binding sites were blocked with Rodent Block M[®] (Biocare Medical), and sections were stained overnight with vimentin at 4°C. The MM-polymer-HRP[®] secondary antibody (Biocare Medical) was used, followed by incubation in diaminobenzidine (Sigma-Aldrich) to visualize vimentin expression. The slides were weakly counterstained with hematoxylin, dehydrated through graded alcohols, and mounted with Permount (VWR International, Amsterdam, The Netherlands).

Ki-67 Staining

A monoclonal mouse antihuman Ki-67 antibody (Clone MIB-1, Cat. No. M7240, Dako) was used to identify actively proliferating cells in cryosections of spheroids and fibrin-based constructs after 7 days of culture. Sections were fixed in acetone for 10 min, washed in PBS, and incubated for 60 min with Ki-67 antibody

(1:200 dilution in PBS/1% BSA) at room temperature. Subsequently, a secondary biotin-conjugated goat anti-mouse antibody (1:200 dilution in PBS/1% BSA, cat no. E0433, Dako) was used for 30 min followed by incubation with streptavidin-horseradish peroxidase (1:300 dilution in PBS/1% BSA, Cat. No. P0397, Dako) for 30 min. Diaminobenzidine (Sigma-Aldrich) was used to visualize Ki-67 expression. The slides were weakly counterstained with hematoxylin, dehydrated through graded alcohols, and mounted with Permount (VWR International). Cell proliferation was quantified on two to three high-resolution (0.23 μ m/pixel), low-magnification (40 \times) digital micrographs (Nanozoomer HT, Hamamatsu Photonics, Hamamatsu City, Japan) covering complete Ki-67-stained cross-sections of each construct using NIH ImageJ software (<http://rsb.info.nih.gov/ij/>). The mitotic index was determined on four fields of view per construct cross-section and calculated as the percentage of Ki-67 positively stained cells to total cells.

Oil Red O Staining

Accumulated lipid in spheroids and fibrin constructs were determined after 7 days of in vitro culture and after 7 days of implantation. In short, a 0.5% (w/v) stock solution of Oil Red O in triethyl-phosphate (Sigma-Aldrich) was diluted 3:2 with deionized water to prepare an Oil Red O working solution. After fixation, cryosections were rinsed in deionized water. Subsequently, the sections were immersed in Oil Red O working solution for 30 min. Hereafter, sections were washed with three exchanges of deionized water for three times. Then sections were counterstained with hematoxylin for 1 min. Finally, sections were rinsed with running tap water for 10 min and covered with Imsolmount (Klinipath, Zevenaar, The Netherlands).

Myeloperoxidase (MPO) Staining

A polyclonal rabbit anti-human MPO antibody (Cat No. A0398, Dako) that cross-reacts with murine myeloperoxidase was used to identify neutrophils in paraffin sections of spheroids and fibrin-based constructs after 7 days of culture. Antigen retrieval was achieved by heating at 95°C for 15 min in Tris/EDTA pH 9.0. Endogenous peroxidase was blocked with 3% H₂O₂ in PBS. The MPO antibody was diluted 1:5,000 with normal antibody diluent (Klinipath, Duiven, The Netherlands), and slides were incubated for 30 min, followed by rinsing with Tris/Tween 0.5%, pH 8.0. Dako ChemMate Envision HRP was applied for 30 min (Dako envision kit), followed by rinsing with Tris/Tween 0.5%, pH 8.0. Diaminobenzidine tetrahydrochloride (Dako envision kit) was applied twice, without rinsing, and rinsed with tap water. Slides were counterstained with hematoxylin for 1 min and rinsed with tap water. Slides were dehydrated through graded

alcohols and mounted with Permount (VWR International B.V., Amsterdam, The Netherlands).

Quantification of Construct Vascularization and Inflammation

H&E staining was performed to evaluate vascularization after implantation. Similarly, MPO staining was performed to evaluate inflammation after implantation. High-resolution (0.23 $\mu\text{m}/\text{pixel}$), low-magnification (40 \times) digital micrographs covering three complete H&E- or MPO-stained cross-sections taken from top, middle, and bottom sections of each retrieved construct were made with a Nanozoomer HT (Hamamatsu Photonics) for analysis.

The rate of vascularization was estimated by counting the total number of vessel lumens per cross-section area using NIH ImageJ software. Vessel lumens were only included when filled with pink-stained, closely packed erythrocytes.

Likewise, the average vessel diameter was determined by measuring the diameter of the vessel lumens in each cross-section. The infiltration of inflammatory cells was scored on a scale from 0 to 3; a score of 0 indicated no or only few inflammatory cells present (minimal inflammation), a score of 1 indicated groups of inflammatory cells around the construct and no or only few cells inside the construct (mild inflammation), a score of 2 indicated groups of inflammatory cells around and inside the construct, and a (severe inflammation) score of 3 indicated inflammatory cells throughout the construct and the surrounding tissue (intense inflammation).

Statistical Analysis

The mitotic indices and all gene expression and protein secretion data were analyzed with the Kruskal–Wallis test followed by post hoc Dunn's multiple comparison tests and are expressed as median (interquartile range, IQR). All vascularization data were analyzed with the unpaired *t* test with Welch correction and are expressed as mean \pm standard deviation. For statistical comparisons of the inflammation scores, the number of spheroids and fibrin-based constructs with scores of 0–1 (indicating minimal to mild inflammation) were compared to the number of spheroids and fibrin constructs with scores of 2–3 (indicating severe to intense inflammation) using the Fisher's exact test. Statistical significance was defined as $p < 0.05$. Statistical analysis was performed using SPSS 15.0 (SPSS, Inc., Chicago, IL, USA).

RESULTS

In Vivo Performance of ASC Tissue Constructs

Following 7 days of culture, spheroids and fibrin-based constructs were implanted subcutaneously in athymic

mice to determine construct *in vivo* engraftment. Seven days after implantation, we could identify eight of nine engrafted spheroids and eight of nine engrafted fibrin-based constructs. There was no variation among ASC donors in retrieval following implantation. Gross examination revealed that both spheroids and fibrin-based constructs had a spherical to oval shape, appeared light yellow in color, and were invaded by vessels (Fig. 1A, B).

H&E-stained cross-sections of the retrieved constructs showed that host blood vessels were present at the periphery of all constructs, while four of eight spheroids and five of eight fibrin-based constructs contained host blood vessels within the constructs (Fig. 1C). To provide more insight in the vascularization of these spheroids and fibrin-based constructs, we determined the number of vessel lumens per cross-section and their average diameter. In fibrin-based constructs, the number of vessel lumens per cross-section (93 ± 45 lumens/ mm^2) was significantly higher when compared to spheroids (23 ± 11 lumens/ mm^2), while the average vessel lumen diameter was comparable (spheroids: 10 ± 2 μm vs. fibrin constructs: 10 ± 1 μm).

H&E-stained cross-sections also showed inflammatory cell infiltration in the retrieved constructs. Since the morphology of the inflammatory cells resembled that of neutrophils, a myeloperoxidase staining was used to score and differentiate the inflammatory cell infiltration of the constructs. A profound neutrophil response, as indicated by a high infiltration of myeloperoxidase-positive cells, was generally noted in cross-sections of spheroids (minimal to mild inflammation: one construct; severe to massive inflammation: seven constructs), whereas the neutrophil response in fibrin construct cross-sections was mainly mild (minimal to mild inflammation: six constructs; severe to intense inflammation: two constructs) (Fig. 2A, B). In addition, immunostaining of construct cross-sections for human vimentin demonstrated no to minor positive staining in the severe to intense inflamed constructs (mainly spheroids), whereas the minimal to mild inflamed constructs (mainly fibrin-based constructs) were strongly positive, indicating that cells of human origin were only sparsely present in the severely inflamed constructs (Fig. 3A). Furthermore, Oil Red O-positive cells were present in the implanted constructs. Notably, Oil Red O-positive staining was confined to areas with human, vimentin-positive cells, as indicated by our stainings in consecutive cross-sections of the same spheroid and fibrin-based constructs (Fig. 3B, C). This finding suggests that these lipid-containing Oil Red O-positive cells are likely from human origin. However, the nature of the Oil Red O staining and the cryosections does not allow us to investigate this at the level of single cells.

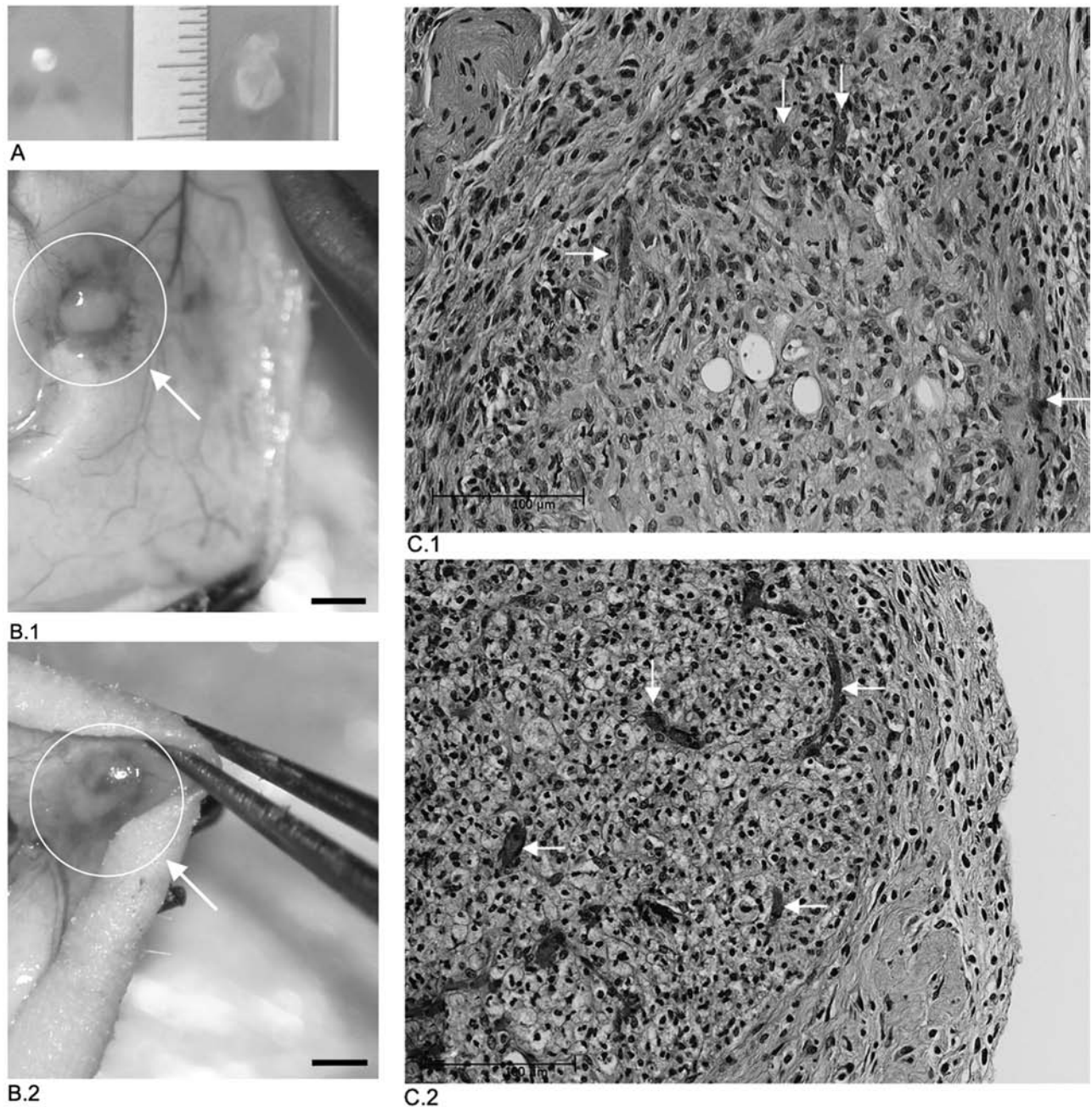


Figure 1. Host blood vessels invade spheroids and fibrin-based constructs. Spheroids and fibrin-based constructs were cultured for 7 days *in vitro* and then implanted subcutaneously in the right and left scapular region of athymic mice for 7 days. Representative images of (A) a spheroid and a fibrin-based construct taken 7 days after culture. Representative images of (B.1) a spheroid and (B.2) a fibrin-based construct taken 7 days after implantation. Scale bars: 1 mm. (C) Construct cross-sections were stained with hematoxylin and eosin. (C.1) Spheroid cross-section and (C.2) fibrin-based construct cross-section, showing invasion of host blood vessels (see white arrows). Scale bars: 100 μm .

Angiogenic Factor Secretion by ASCs in Spheroids and Fibrin-Based Constructs

The ability of ASCs to secrete angiogenic factors may have beneficial effects on the vascularization and survival of ASC constructs *in vivo*. To assess the ability of ASCs to secrete angiogenic factors, we analyzed the release of several

angiogenic factors into the culture medium over a 48-h period. Figure 4 illustrates the data from several important angiogenic factors assayed by multiplex chemiluminescent ELISA at day 7. Of these, FGF2 was added to the culture medium, which masks any differences in the levels of FGF2 between the conditioned media and unconditioned medium.

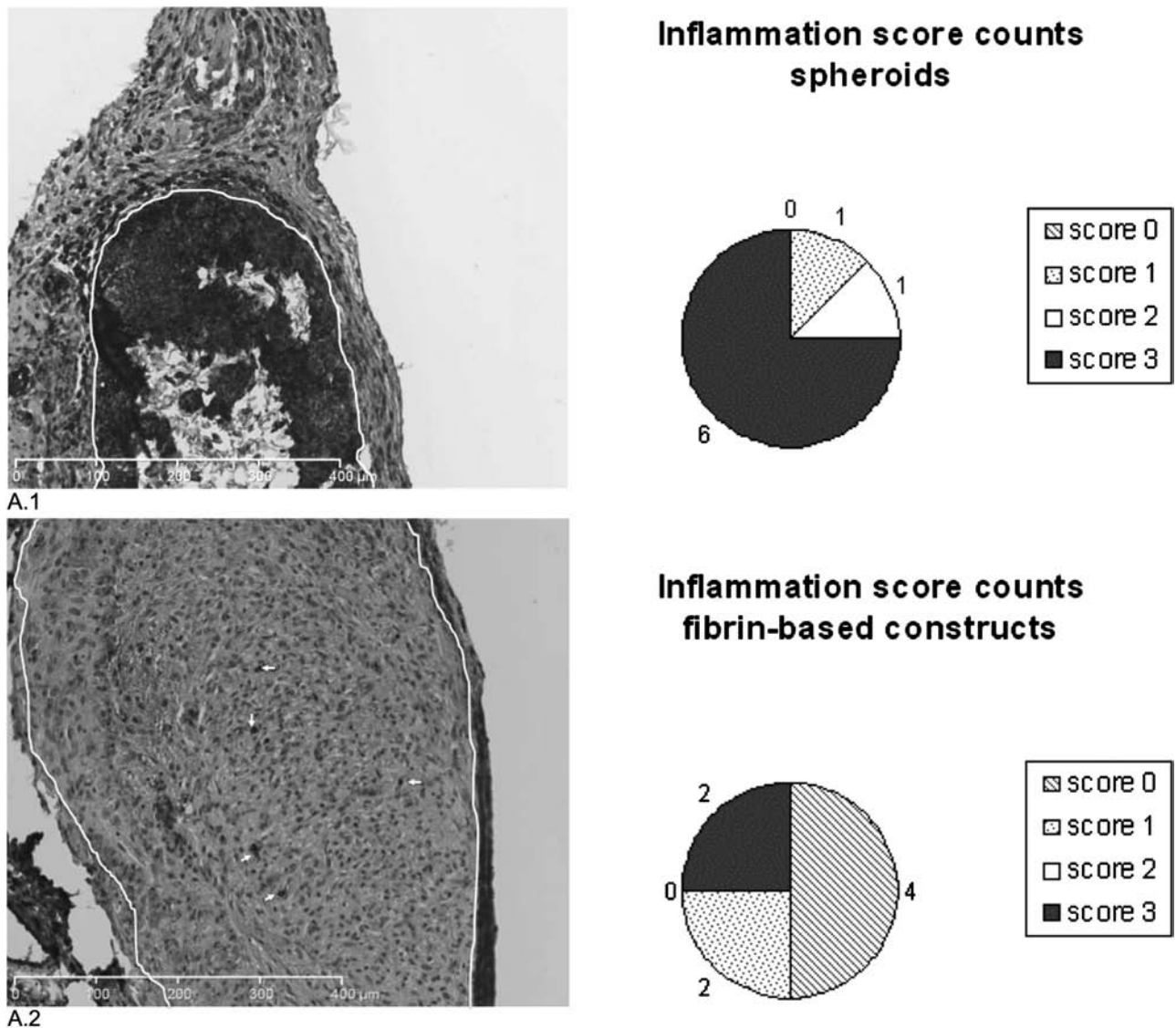


Figure 2. Upon 7 days of implantation fibrin-based constructs elicit a less severe inflammatory response than spheroids. Representative images (A) of myeloperoxidase-stained cross-sections of (A.1) a spheroid and (A.2) a fibrin-based construct after 7 days of implantation in athymic mice. The areas covered by the spheroid and fibrin-based construct (see white line) are indicated. (A.1) The spheroid construct is infiltrated by stained myeloperoxidase-positive cells and shows resorption in the center of the construct cross-section. (A.2) Positively stained cells in the fibrin-based construct are indicated (see arrows). Some light staining is seen where diaminobenzidine sticks to the fibrin gel. Scale bars: 400 μm. (B) Scoring of the inflammatory response to the constructs. High inflammatory response to spheroids (score 0–1 = minimum to mild inflammation; 1 construct, score 2–3 = severe to intense inflammation; 7 constructs) was noted while the inflammatory response to fibrin-based constructs was grossly mild (score 0–1 = minimum to mild inflammation; 6 constructs, score 2–3 = severe to intense inflammation; 2 constructs).

No significant differences in the levels of ANG2 and PDGF between conditioned and unconditioned medium were observed. In contrast, the levels of TIMP2 in conditioned medium from fibrin constructs and the levels of TIMP1 in conditioned medium from both spheroids and fibrin-based constructs were significantly higher when compared to unconditioned medium. Moreover, the levels of HGF and VEGF in conditioned medium from fibrin-based constructs were significantly higher when

compared to spheroid conditioned and unconditioned medium. ASCs from different donors gave similar results regarding angiogenic factor secretion in spheroids and fibrin-based constructs.

Inflammatory Cytokine Secretion by ASCs in Spheroids and Fibrin-Based Constructs

The secretion of a vast amount of proinflammatory cytokines may have a negative effect on the in vivo

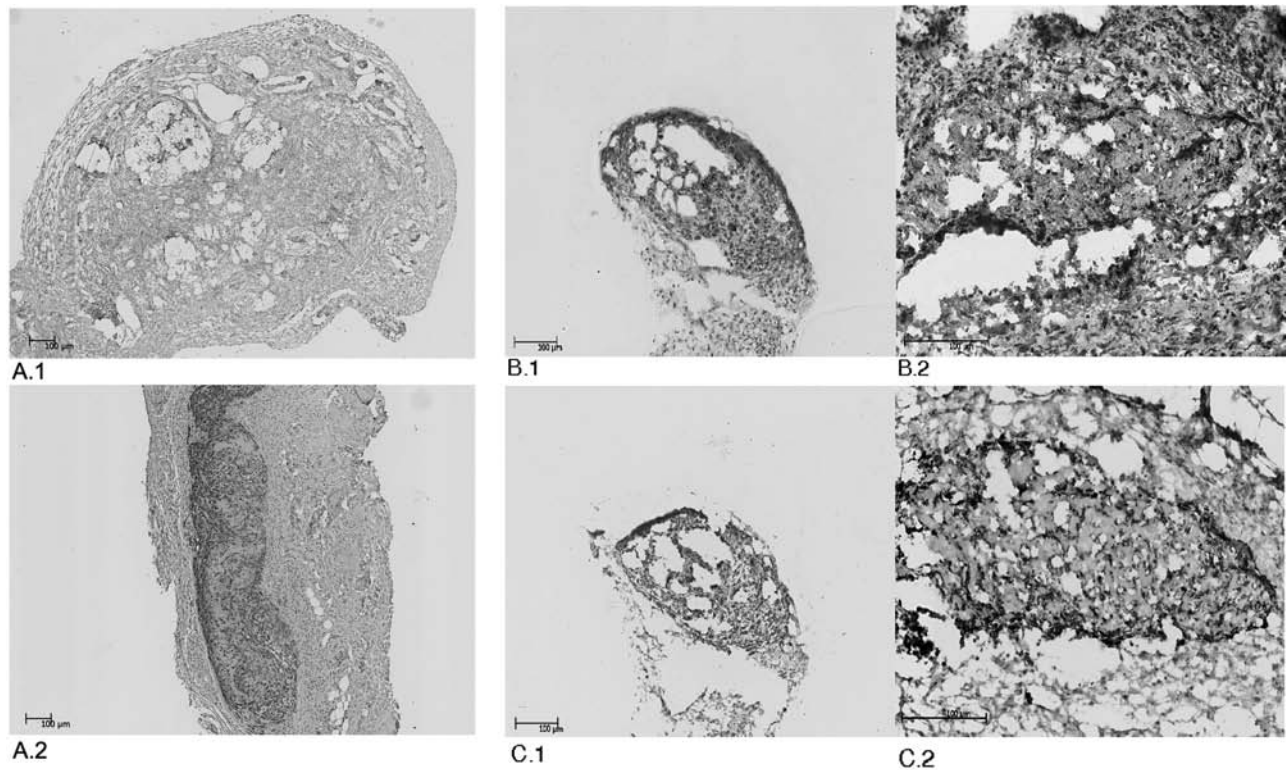


Figure 3. Assessment of ASC presence and lipid accumulation in transplanted spheroids and fibrin-based constructs. To detect adipose-derived stromal cells (ASCs) in spheroids and fibrin-based constructs after 7 days of implantation, cross-sections were stained with human specific vimentin antibody and counterstained with haematoxylin. (A) Representative images of antihuman vimentin-stained cross-sections of a spheroid (A.1) and a fibrin-based construct (A.2) after 7 days of implantation. Note the limited vimentin staining in the inflamed spheroid when compared to the fibrin-based construct. (B) To detect lipid accumulation in constructs after 7 days of implantation, cross-sections were stained with Oil Red O and counterstained with haematoxylin. (B.1) Spheroid and (B.2) fibrin-based construct. (C) Antihuman vimentin-stained consecutive cross-section of the same spheroid (C.1) and fibrin-based construct (C.2) as shown in (B.1) and (B.2). Note that Oil Red O-positive cells and vimentin-positive cells coincide in the same area. Scale bars: 100 μ m.

engraftment of ASC constructs. To assess if culture of ASCs in spheroids or fibrin-based constructs modulated the secretion of inflammatory cytokines, we analyzed the release of several inflammatory cytokines into the culture medium over a 48-h period. Figure 5 illustrates the data from nine different proteins assayed by multiplex chemiluminescent ELISA at day 7. No statistically significant differences in the secretion of the cytokines IL-1 α , IL-2, IL-4, and IL-10 were observed between conditioned media of spheroids and fibrin-based constructs when compared to unconditioned medium (=control). In contrast, IL-1 β , IL-6, IFN- γ , and TNF- α were secreted in significant amounts in both spheroids and fibrin-based constructs when compared to unconditioned medium. In addition, the levels of IL-8 in spheroid conditioned medium were significantly higher when compared to conditioned medium from fibrin-based constructs and unconditioned medium. The ASCs of different donors gave similar results regarding cytokine secretion in spheroids and fibrin-based constructs.

ASC Adipogenic Differentiation in Spheroids and Fibrin-Based Constructs

Previous studies have shown that adipogenic differentiation of ASCs *in vitro* can improve adipogenesis *in vivo* (8,55). Important characteristics of adipogenic differentiation are the accumulation of lipid, the expression of adipogenesis-related markers, and the secretion of leptin (17,28). To determine lipid accumulation in ASCs in spheroids and fibrin-based constructs after 7 days of culture, we stained cryosections with Oil Red O. Oil Red O-positive cells were evident in both spheroids and fibrin-based constructs (Fig. 6A). Unfortunately, due to the high density of cells in especially the spheroid construct cross-sections, it was impossible to accurately determine the amount and size of the lipid droplets in the constructs. Therefore, the Oil Red O staining could not be used to quantitate lipid accumulation in spheroids and fibrin-based constructs.

To quantitatively assess adipogenic differentiation of the ASCs in spheroids and fibrin-based constructs, we

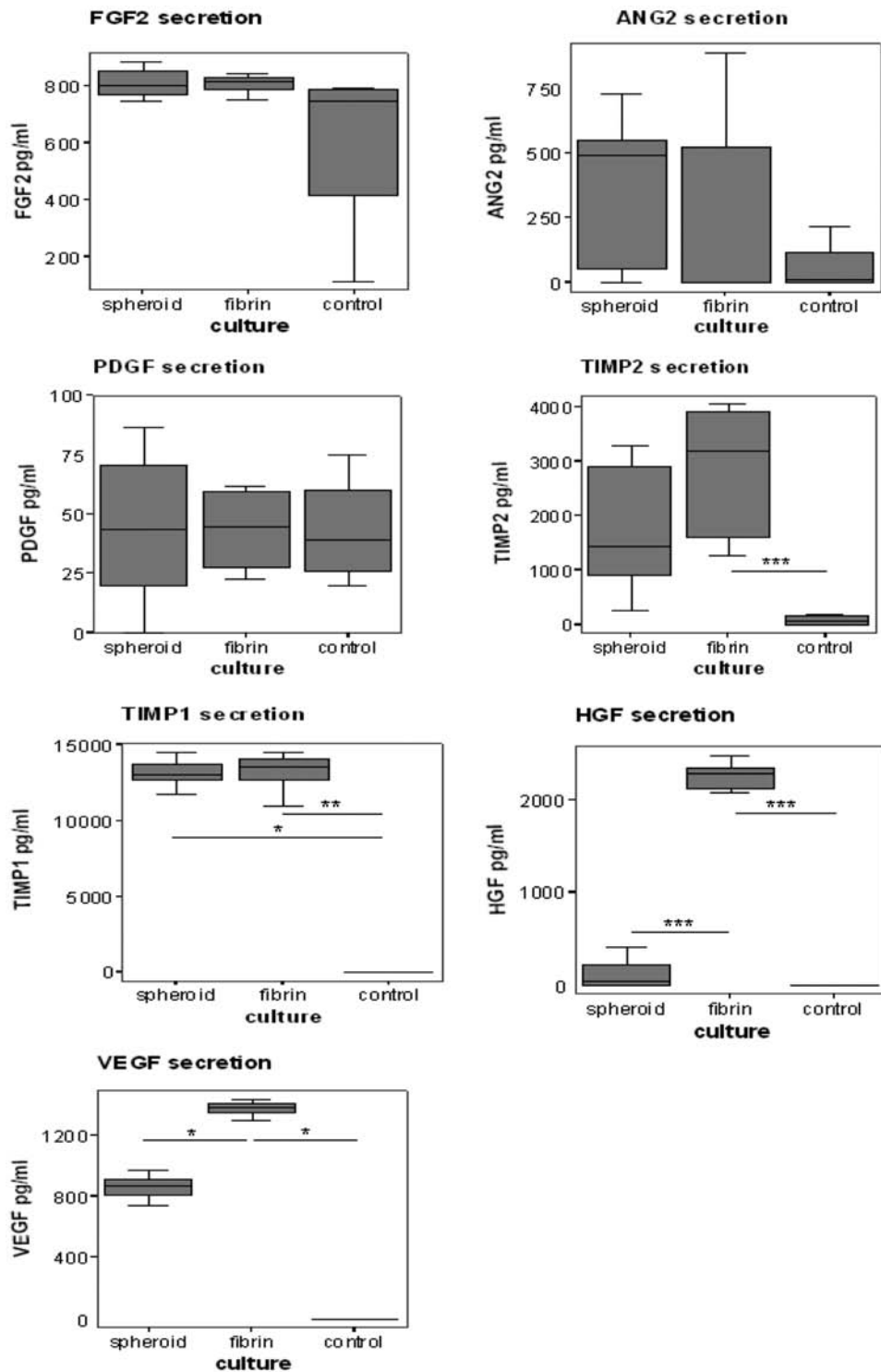
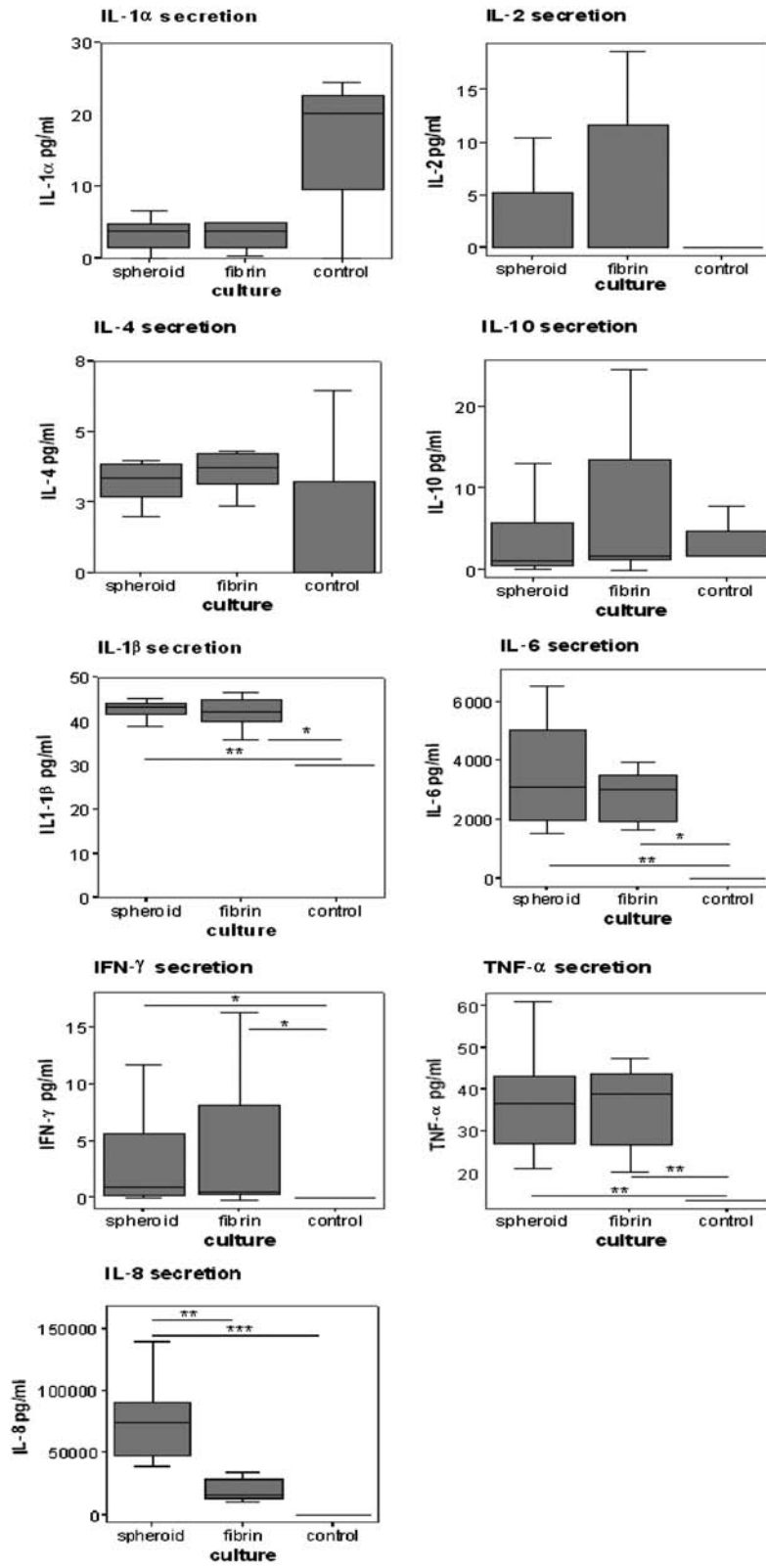


Figure 4. ASCs in fibrin-based constructs secrete higher levels of the angiogenic factors VEGF and HGF than ASC in spheroids. The secretion of the angiogenic factors fibroblast growth factor 2 (FGF2), angiopoietin (ANG2), platelet-derived growth factor (PDGF), tissue inhibitors of matrix metalloproteinases 2 (TIMP2), TIMP1, hepatocyte growth factor (HGF), and vascular endothelial growth factor (VEGF) by ASCs in spheroids and fibrin-based constructs over 48 h was measured by multiplex chemiluminescent ELISA at day 7. Unconditioned adipogenic medium was used as control condition. Values are presented as median (interquartile range); $n=5$, 3 ASC donors. * $p \leq 0.05$, ** $p \leq 0.01$, *** $p \leq 0.001$ (fibrin-based construct conditioned medium vs. spheroid conditioned medium and control).



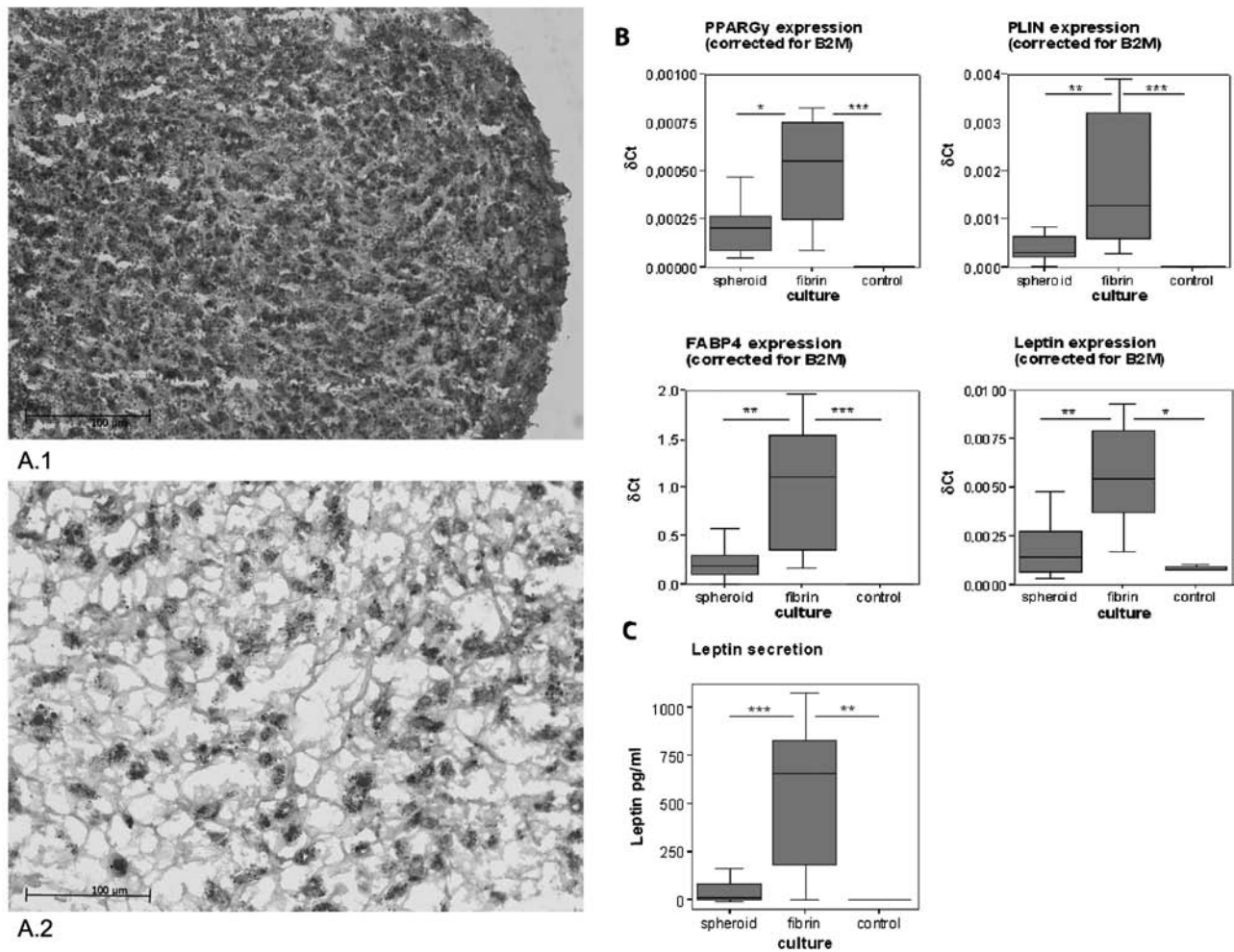


Figure 6. ASCs in fibrin-based constructs display increased adipogenic differentiation when compared to ASCs in spheroids. (A) ASCs in spheroids and fibrin-based constructs were cultured for 7 days in vitro in adipogenic medium. Cross-sections were stained with Oil Red O (showing intracellular lipid) and counterstained with haematoxylin. (A.1) Spheroid. (A.2) Fibrin-based construct. Scale bars: 100 μ m. (B) Q-PCR was used to measure the expression levels of the adipocyte-specific markers peroxisome proliferator-activated receptor γ (PPARG), perilipin 1 (PLIN 1), fatty acid binding protein 4 (FABP4), and leptin (LEP). Expression levels are relative to β -2-microglobulin-positive control housekeeping gene (δ Ct). Values are presented as medians (interquartile range). For each of the three ASC donors, nine spheroids, nine fibrin-based constructs, and 0.5×10^6 undifferentiated ASCs (=control) were prepared and assayed. $*p \leq 0.05$, $**p \leq 0.01$, and $***p \leq 0.001$ (relative expression in fibrin-based constructs compared to spheroids and control). (C) The secretion of leptin by ASCs in conditioned medium of spheroids and fibrin-based constructs over 48 h was measured by sandwich ELISA at day 7. Unconditioned adipogenic medium was used as control condition. Values are presented as median (interquartile range); $n=9$, 3 ASC donors. $**p \leq 0.01$, $***p \leq 0.001$ (fibrin-based construct conditioned medium vs. spheroid conditioned medium and control).

measured the gene expression of the four adipogenic markers, PPARG, PLIN1, FABP4, and LEP, after 7 days of culture. In addition, we measured the release of the adipocyte-specific protein leptin into the culture medium over a 48-h period. Q-PCR analysis showed that all four

adipogenic markers were expressed in ASC cultured in spheroids or fibrin-based constructs. Notably, only ASCs in fibrin-based constructs showed a significantly higher expression of these adipogenic markers when compared to undifferentiated ASCs harvested at day 0 (=control)

FACING PAGE

Figure 5. ASCs in fibrin-based constructs secrete lower levels of the cytokine interleukin-8 than ASCs in spheroids. The secretion of the inflammatory cytokines interleukin-1 α (IL-1 α), IL-2, IL-4, IL-10, IL-1 β , IL-6, tumor necrosis factor (TNF)- α , interferon (IFN)- γ , and IL-8 by ASCs in spheroids and fibrin-based constructs over 48 h was measured by multiplex chemiluminescent ELISA at day 7. Unconditioned adipogenic medium was used as control condition. Values are presented as median (interquartile range); $n=5$, 3 ASC donors. $*p \leq 0.05$, $**p \leq 0.01$, $***p \leq 0.001$ (spheroid and fibrin-based construct conditioned medium vs. each other and control).

(Fig. 6B). Moreover, the levels of leptin in conditioned medium from fibrin-based constructs were significantly higher when compared to conditioned medium from spheroids and unconditioned medium (=control) (Fig. 6C). No ASC donor-related differences regarding adipogenic differentiation of ASCs in spheroids and fibrin-based constructs were observed.

To determine the proliferative activity of differentiating ASCs in spheroid and fibrin-based constructs, Ki-67 staining was used. Mitotic indices were calculated.

Comparison of the mitotic index revealed no significant difference in ASC proliferative activity between spheroids and fibrin-based constructs (spheroid mitotic index median: 3% [IQR: 9.7–1.1%] vs. fibrin median: 3.5% [IQR: 8.9–0.7%]).

DISCUSSION

The results of our study suggest that fibrin-based ASC constructs better support *in vivo* engraftment than scaffold-free ASC spheroids, as indicated by a less severe inflammatory response and a higher degree of vascularization after *in vivo* transplantation. In addition, fibrin-based ASC constructs better support ASC adipogenesis as indicated by the higher expression levels of adipocyte-specific markers and the increased secretion of leptin.

An important parameter determining the success of ASC constructs for soft tissue repair is an unfavorable host response. In our study, the inflammatory response after subcutaneous transplantation in nude mice was more profound in spheroids than that in fibrin-based constructs. In line with this finding, ASCs cultured in spheroids secreted higher amounts of the proinflammatory mediator IL-8 than ASCs cultured in fibrin-based constructs. Taken together, these findings indicate that the ASCs in spheroids induce a higher inflammatory response than ASCs in fibrin-based constructs, which likely results from a higher secretion of IL-8. However, the possibility that other than the investigated factors contributed to the higher inflammatory response in spheroids, such as more cell death due to less sufficient diffusion of oxygen and nutrients, cannot be ruled out yet.

Another important parameter determining the success of ASC constructs is vascularization (31,38,59). We quantified the vascularization of construct cross-sections upon transplantation and found that the number of vascular lumens-per-construct area was significantly higher in fibrin-based constructs when compared to spheroids, indicating augmented ingrowth of mouse vessels. As well as being an important chemoattractant for inflammatory cells, IL-8 is also known to be angiogenic. Although ASCs in spheroids secreted IL-8 more than the fibrin implants in our experiments, other prominent proangiogenic factors, such as VEGF and HGF, were secreted

in higher amounts by ASCs in fibrin-based constructs when compared to spheroids. This may explain why less blood vessel ingrowth was seen in spheroids compared to fibrin-based constructs. In all, these findings indicate that fibrin favors the vascularization of ASC constructs upon transplantation. Such a positive effect of fibrin on *in vivo* vascularization has also recently been shown for bone marrow-derived stromal cell/fibrin-based constructs by Huang et al. (23).

Although previous studies demonstrate that scaffold-free spheroid culture provides favorable conditions for reconstruction of liver (30), pancreas (35), blood vessel (29), myocardial muscle (26), ganglion (26), cartilage (34), and bone tissue (2,44), its use for reconstruction of adipose tissue has not been investigated until now. Determination of ASC adipogenic differentiation is complex and should be investigated by more than one method. Therefore, we determined lipid accumulation using Oil Red O staining and investigated the expression levels of four adipocyte-specific genes as well as the secretion of the adipocyte-specific protein leptin. Although both ASC spheroids and ASC fibrin-based constructs contained Oil Red O-positive lipid droplets, all adipocyte-specific genes were upregulated in ASC fibrin-based constructs when compared to ASC spheroids. Besides that, also the secretion of leptin was significantly higher in fibrin-based constructs when compared to spheroids. Since the upregulation of four adipocyte-specific genes together with a higher secretion of leptin is very likely to be related to ASC conversion to adipocytes, our results suggest that adipogenic differentiation of ASCs is increased in fibrin-based cultures when compared to scaffold-free spheroid cultures. Therefore, we conclude that the spheroid culture environment is less favorable for ASC adipogenic differentiation than the fibrin culture environment. Possibly, differences in cell density accounted for the observed differences in ASC adipogenic differentiation between spheroid and fibrin-based cultures. In fibrin-based cultures, ASCs are more loosely packed than in the spheroid cultures, as can be seen in Figure 6A, B. Mueller-Klieser et al. (39) and others (7,15) showed that the relatively high cell density of especially larger (>150–200 μm) spheroids limits the diffusion of many molecules to individual cells inside the spheroids, leading to nutrient deprivation. It could therefore be hypothesized that the observed difference in adipogenic differentiation between spheroids and fibrin-based cultures are due to a difference in nutrient delivery to individual cells.

Collectively, our *in vitro* and *in vivo* experiments with fibrin are promising and demonstrate that fibrin provides favorable conditions for adipose tissue reconstruction. Before clinical application, future studies should

determine the long-term in vivo survival of fibrin-based adipose constructs, as well as attempt to develop fibrin-based adipose constructs of appropriate size and predictable forms to repair soft tissue defects.

A potential strategy that could benefit the in vivo survival of especially larger fibrin-based adipose constructs is the prefabrication of a vascular network within the tissue construct, as previously demonstrated by Levenberg et al. (32) for engineered skeletal muscle tissue. Furthermore, advanced techniques, such as inkjet printing and magnetically influenced self-assembly, can be used to alter the geometry of the fibrin-based constructs into appropriate and predictable forms (1,3,37,56).

CONCLUSIONS

The use of fibrin-based ASC constructs leads to increased expression of adipocyte-specific markers, a higher secretion of angiogenic factors, and a lower secretion of the cytokine IL-8 when compared to scaffold-free ASC spheroids. In addition, fibrin-based ASC constructs display a higher degree of vascularization and elicit a less severe inflammatory response than ASC spheroids upon short-term transplantation. These results indicate that fibrin-based constructs are potentially more suitable for ASC-based adipose tissue reconstruction than scaffold-free ASC spheroids. Furthermore, long-term in vivo studies are, however, needed before fibrin-based ASC constructs can be used in soft tissue repair.

ACKNOWLEDGMENTS: This work was supported by the NutsOhra Foundation (contract no. SNO-T-07-75). The authors wish to thank Suzanne Reneman, Vincent Vaes, and Corinna de Ridder for their assistance with the in vivo experiments, the Department of Pathology for the use of the Nanozoomer HT, and René van den Ham for careful review of this manuscript. The authors declare no conflicts of interest.

REFERENCES

- Ahmed, T. A.; Dare, E. V.; Hincke, M. Fibrin: A versatile scaffold for tissue engineering applications. *Tissue Eng. Part B Rev.* 14(2):199–215; 2008.
- Akiyama, M.; Nonomura, H.; Kamil, S. H.; Ignatz, R. A. Periosteal cell pellet culture system: A new technique for bone engineering. *Cell Transplant.* 15(6):521–532; 2006.
- Alsberg, E.; Feinstein, E.; Joy, M. P.; Prentiss, M.; Ingber, D. E. Magnetically-guided self-assembly of fibrin matrices with ordered nano-scale structure for tissue engineering. *Tissue Eng.* 12(11):3247–3256; 2006.
- Alster, T. S.; West, T. B. Human-derived and new synthetic injectable materials for soft-tissue augmentation: Current status and role in cosmetic surgery. *Plast. Reconstr. Surg.* 105(7):2515–2525; 2000.
- Bell, L. N.; Cai, L.; Johnstone, B. H.; Traktuev, D. O.; March, K. L.; Considine, R. V. A central role for hepatocyte growth factor in adipose tissue angiogenesis. *Am. J. Physiol. Endocrinol. Metab.* 294(2):E336–344; 2008.
- Billings, Jr., E.; May, Jr., J. W. Historical review and present status of free fat graft autotransplantation in plastic and reconstructive surgery. *Plast. Reconstr. Surg.* 83(2):368–381; 1989.
- Carlsson, J.; Acker, H. Relations between pH, oxygen partial pressure and growth in cultured cell spheroids. *Int. J. Cancer* 42(5):715–720; 1988.
- Cho, S. W.; Kim, I.; Kim, S. H.; Rhie, J. W.; Choi, C. Y.; Kim, B. S. Enhancement of adipose tissue formation by implantation of adipogenic-differentiated preadipocytes. *Biochem. Biophys. Res. Commun.* 345(2):588–594; 2006.
- Cho, S. W.; Kim, S. S.; Rhie, J. W.; Cho, H. M.; Choi, C. Y.; Kim, B. S. Engineering of volume-stable adipose tissues. *Biomaterials* 26(17):3577–3585; 2005.
- Cho, S. W.; Song, K. W.; Rhie, J. W.; Park, M. H.; Choi, C. Y.; Kim, B. S. Engineered adipose tissue formation enhanced by basic fibroblast growth factor and a mechanically stable environment. *Cell Transplant.* 16(4):421–434; 2007.
- Choi, Y. S.; Park, S. N.; Suh, H. Adipose tissue engineering using mesenchymal stem cells attached to injectable PLGA spheres. *Biomaterials* 26(29):5855–5863; 2005.
- Coleman, S. R. Facial recontouring with lipostucture. *Clin. Plast. Surg.* 24(2):347–367; 1997.
- Coleman, S. R. Long-term survival of fat transplants: Controlled demonstrations. *Aesthetic Plast. Surg.* 19(5):421–425; 1995.
- Cukierman, E.; Pankov, R.; Yamada, K. M. Cell interactions with three-dimensional matrices. *Curr. Opin. Cell Biol.* 14(5):633–639; 2002.
- Curcio, E.; Salerno, S.; Barbieri, G.; De Bartolo, L.; Drioli, E.; Bader, A. Mass transfer and metabolic reactions in hepatocyte spheroids cultured in rotating wall gas-permeable membrane system. *Biomaterials* 28(36):5487–5497; 2007.
- Fischbach, C.; Spruss, T.; Weiser, B.; Neubauer, M.; Becker, C.; Hacker, M.; Gopferich, A.; Blunk, T. Generation of mature fat pads in vitro and in vivo utilizing 3-D long-term culture of 3T3-L1 preadipocytes. *Exp. Cell Res.* 300(1):54–64; 2004.
- Gregoire, F. M. Adipocyte differentiation: From fibroblast to endocrine cell. *Exp. Biol. Med.* 226(11):997–1002; 2001.
- Halberstadt, C.; Austin, C.; Rowley, J.; Culberson, C.; Loebbeck, A.; Wyatt, S.; Coleman, S.; Blacksten, L.; Burg, K.; Mooney, D.; Holder, Jr., W. A hydrogel material for plastic and reconstructive applications injected into the subcutaneous space of a sheep. *Tissue Eng.* 8(2):309–319; 2002.
- Hart, D. Overcoming complications of breast implants. *Plast. Surg. Nurs.* 23(2):55–63, 72; 2003.
- Hemrich, K.; Van de Sijpe, K.; Rhodes, N. P.; Hunt, J. A.; Di Bartolo, C.; Pallua, N.; Blondeel, P.; von Heimburg, D. Autologous in vivo adipose tissue engineering in hyaluronan-based gels—A pilot study. *J. Surg. Res.* 144(1):82–88; 2008.
- Hemrich, K.; von Heimburg, D. Biomaterials for adipose tissue engineering. *Expert Rev. Med. Devices* 3(5):635–645; 2006.
- Hemrich, K.; von Heimburg, D.; Rendchen, R.; Di Bartolo, C.; Milella, E.; Pallua, N. Implantation of preadipocyte-loaded hyaluronic acid-based scaffolds into nude mice to evaluate potential for soft tissue engineering. *Biomaterials* 26(34):7025–7037; 2005.
- Huang, N. F.; Lam, A.; Fang, Q.; Sievers, R. E.; Li, S.; Lee, R. J. Bone marrow-derived mesenchymal stem cells in fibrin augmented angiogenesis in the chronically infarcted myocardium. *Regen. Med.* 4(4):527–538; 2009.

24. Kawaguchi, N.; Toriyama, K.; Nicodemou-Lena, E.; Inou, K.; Torii, S.; Kitagawa, Y. De novo adipogenesis in mice at the site of injection of basement membrane and basic fibroblast growth factor. *Proc. Natl. Acad. Sci. USA* 95(3):1062–1066; 1998.
25. Kelm, J. M.; Fussenegger, M. Microscale tissue engineering using gravity-enforced cell assembly. *Trends Biotechnol.* 22(4):195–202; 2004.
26. Kelm, J. M.; Timmins, N. E.; Brown, C. J.; Fussenegger, M.; Nielsen, L. K. Method for generation of homogeneous multicellular tumor spheroids applicable to a wide variety of cell types. *Biotechnol. Bioeng.* 83(2):173–180; 2003.
27. Kimura, Y.; Ozeki, M.; Inamoto, T.; Tabata, Y. Adipose tissue engineering based on human preadipocytes combined with gelatin microspheres containing basic fibroblast growth factor. *Biomaterials* 24(14):2513–2521; 2003.
28. Klimcakova, E.; Moro, C.; Mazzucotelli, A.; Lolmede, K.; Viguerie, N.; Galitzky, J.; Stich, V.; Langin, D. Profiling of adipokines secreted from human subcutaneous adipose tissue in response to PPAR agonists. *Biochem. Biophys. Res. Commun.* 358(3):897–902; 2007.
29. Korff, T.; Augustin, H. G. Integration of endothelial cells in multicellular spheroids prevents apoptosis and induces differentiation. *J. Cell Biol.* 143(5):1341–1352; 1998.
30. Landry, J.; Bernier, D.; Ouellet, C.; Goyette, R.; Marceau, N. Spheroidal aggregate culture of rat liver cells: Histotypic reorganization, biomatrix deposition, and maintenance of functional activities. *J. Cell Biol.* 101(3):914–923; 1985.
31. Laschke, M. W.; Harder, Y.; Amon, M.; Martin, I.; Farhadi, J.; Ring, A.; Torio-Padron, N.; Schramm, R.; Rucker, M.; Junker, D.; Häufel, J. M.; Carvalho, C.; Heberer, M.; Germann, G.; Vollmar, B.; Menger, M. D. Angiogenesis in tissue engineering: Breathing life into constructed tissue substitutes. *Tissue Eng.* 12(8):2093–2104; 2006.
32. Levenberg, S.; Rouwkema, J.; Macdonald, M.; Garfein, E. S.; Kohane, D. S.; Darland, D. C.; Marini, R.; van Blitterswijk, C. A.; Mulligan, R. C.; D'Amore, P. A.; Langer, R. Engineering vascularized skeletal muscle tissue. *Nat. Biotechnol.* 23(7):879–884; 2005.
33. Lorenz, H. P.; Hedrick, M. H.; Chang, J.; Mehrara, B. J.; Longaker, M. T. The impact of biomolecular medicine and tissue engineering on plastic surgery in the 21st century. *Plast. Reconstr. Surg.* 105(7):2467–2481; 2000.
34. Martinez, I.; Elvenes, J.; Olsen, R.; Bertheussen, K.; Johansen, O. Redifferentiation of in vitro expanded adult articular chondrocytes by combining the hanging-drop cultivation method with hypoxic environment. *Cell Transplant.* 17(8):987–996; 2008.
35. Matta, S. G.; Wobken, J. D.; Williams, F. G.; Bauer, G. E. Pancreatic islet cell reaggregation systems: Efficiency of cell reassociation and endocrine cell topography of rat islet-like aggregates. *Pancreas* 9(4):439–449; 1994.
36. McGlohorn, J. B.; Grimes, L. W.; Webster, S. S.; Burg, K. J. Characterization of cellular carriers for use in injectable tissue-engineering composites. *J. Biomed. Mater. Res.* A 66(3):441–449; 2003.
37. Mironov, V.; Boland, T.; Trusk, T.; Forgacs, G.; Markwald, R. R. Organ printing: Computer-aided jet-based 3D tissue engineering. *Trends Biotechnol.* 21(4):157–161; 2003.
38. Mooney, D. J.; Mikos, A. G. Growing new organs. *Sci. Am.* 280(4):60–65; 1999.
39. Mueller-Klieser, W. Multicellular spheroids. A review on cellular aggregates in cancer research. *J. Cancer Res. Clin. Oncol.* 113(2):101–122; 1987.
40. Neuss, S.; Stainforth, R.; Salber, J.; Schenck, P.; Bovi, M.; Knuchel, R.; Perez-Bouza, A. Long-term survival and bipotent terminal differentiation of human mesenchymal stem cells (hMSC) in combination with a commercially available three-dimensional collagen scaffold. *Cell Transplant.* 17(8):977–986; 2008.
41. Niechajev, I.; Sevcuk, O. Long-term results of fat transplantation: Clinical and histologic studies. *Plast. Reconstr. Surg.* 94(3):496–506; 1994.
42. Patrick, Jr., C. W.; Chauvin, P. B.; Hopley, J.; Reece, G. P. Preadipocyte seeded PLGA scaffolds for adipose tissue engineering. *Tissue Eng.* 5(2):139–151; 1999.
43. Patrick, Jr., C. W.; Zheng, B.; Johnston, C.; Reece, G. P. Long-term implantation of preadipocyte-seeded PLGA scaffolds. *Tissue Eng.* 8(2):283–293; 2002.
44. Rouwkema, J.; de Boer, J.; Van Blitterswijk, C. A. Endothelial cells assemble into a 3-dimensional prevascular network in a bone tissue engineering construct. *Tissue Eng.* 12(9):2685–2693; 2006.
45. Schoeller, T.; Lille, S.; Wechselberger, G.; Otto, A.; Mowlavi, A.; Piza-Katzer, H. Histomorphologic and volumetric analysis of implanted autologous preadipocyte cultures suspended in fibrin glue: A potential new source for tissue augmentation. *Aesthetic Plast. Surg.* 25(1):57–63; 2001.
46. Stacey, D. H.; Hanson, S. E.; Lahvis, G.; Gutowski, K. A.; Masters, K. S. In vitro adipogenic differentiation of preadipocytes varies with differentiation stimulus, culture dimensionality, and scaffold composition. *Tissue Eng. Part A* 15(11):3389–3399; 2009.
47. Stevens, K. R.; Pabon, L.; Muskheli, V.; Murry, C. E. Scaffold-free human cardiac tissue patch created from embryonic stem cells. *Tissue Eng. Part A* 15(6):1211–1222; 2009.
48. Stosich, M. S.; Mao, J. J. Adipose tissue engineering from human adult stem cells: Clinical implications in plastic and reconstructive surgery. *Plast. Reconstr. Surg.* 119(1):71–83; discussion 84–85; 2007.
49. Torio-Padron, N.; Baerlecken, N.; Momeni, A.; Stark, G. B.; Borges, J. Engineering of adipose tissue by injection of human preadipocytes in fibrin. *Aesthetic Plast. Surg.* 31(3):285–293; 2007.
50. Vallee, M.; Cote, J. F.; Fradette, J. Adipose-tissue engineering: Taking advantage of the properties of human adipose-derived stem/stromal cells. *Pathol. Biol.* 57(4):309–317; 2009.
51. Vermette, M.; Trottier, V.; Menard, V.; Saint-Pierre, L.; Roy, A.; Fradette, J. Production of a new tissue-engineered adipose substitute from human adipose-derived stromal cells. *Biomaterials* 28(18):2850–2860; 2007.
52. Verseijden, F.; Jahr, H.; Posthumus-van Sluijs, S. J.; Ten Hagen, T. L.; Hovius, S. E.; Seynhaeve, A. L.; van Neck, J. W.; van Osch, G. J.; Hofer, S. O. Angiogenic capacity of human adipose-derived stromal cells during adipogenic differentiation: An in vitro study. *Tissue Eng. Part A* 15(2):445–452; 2009.
53. Verseijden, F.; Sluijs, S. P.; Farrell, E.; van Neck, J.; Hovius, S.; Hofer, S.; van Osch, G. Prevascular structures promote vascularization in engineered human adipose tissue constructs upon implantation. *Cell Transplant.* 19(8):1007–1020; 2010.
54. Wechselberger, G.; Russell, R. C.; Neumeister, M. W.; Schoeller, T.; Piza-Katzer, H.; Rainer, C. Successful

- transplantation of three tissue-engineered cell types using capsule induction technique and fibrin glue as a delivery vehicle. *Plast. Reconstr. Surg.* 110(1):123–129; 2002.
55. Weiser, B.; Prantl, L.; Schubert, T. E.; Zellner, J.; Fischbach-Teschl, C.; Spruss, T.; Seitz, A. K.; Tessmar, J.; Goepferich, A.; Blunk, T. In vivo development and long-term survival of engineered adipose tissue depend on in vitro precultivation strategy. *Tissue Eng. Part A* 14(2):275–284; 2008.
56. Xu, T.; Gregory, C. A.; Molnar, P.; Cui, X.; Jalota, S.; Bhaduri, S. B.; Boland, T. Viability and electrophysiology of neural cell structures generated by the inkjet printing method. *Biomaterials* 27(19):3580–3588; 2006.
57. Yang, S.; Leong, K. F.; Du, Z.; Chua, C. K. The design of scaffolds for use in tissue engineering. Part I. Traditional factors. *Tissue Eng.* 7(6):679–689; 2001.
58. Ye, Q.; Zund, G.; Benedikt, P.; Jockenhoewel, S.; Hoerstrup, S. P.; Sakyama, S.; Hubbell, J. A.; Turina, M. Fibrin gel as a three dimensional matrix in cardiovascular tissue engineering. *Eur. J. Cardiothorac. Surg.* 17(5):587–591; 2000.
59. Zandonella, C. Tissue engineering: The beat goes on. *Nature* 421(6926):884–886; 2003.